Calcif Tissue Int (1996) 59:58–63

Calcified Tissue International

X-Ray Diffraction, Electron Microscopy, and Fourier Transform Infrared Spectroscopy of Apatite Crystals Isolated From Chicken and Bovine Calcified Cartilage

H.-M. Kim,* C. Rey, M. J. Glimcher

Laboratory for the Study of Skeletal Disorders and Rehabilitation, Department of Orthopaedic Surgery, Enders Building, Room 1116, 300 Longwood Avenue, Harvard Medical School, Children's Hospital, Boston, Massachusetts 02115, USA

Received: 1 December 1995 / Accepted: 12 February 1996

Abstract. Apatite crystals of the calcified zone of the subarticular cartilaginous growth plates of the long bones of young growing chickens and calves were isolated by low temperature reaction with hydrazine and plasma ashing and examined by electron microscopy, electron diffraction and microprobe analysis, and computer-generated deconvolution of the spectra obtained by Fourier transform infrared spectroscopy. The crystal habit was that of wide, very thin, relatively long rectangular plates, which tended to form small clusters of crystals, possibly because reaction with hydrazine alone did not remove all of the organic matrix constituents. Further reaction with low power plasma ashing released more of the isolated crystals although to a lesser extent than was possible with bone. Stereograms of the small clusters showed that many of the crystals in the small isolated aggregates of crystals were bent and/or curved. Together with the resultant overlap of individual adjacent crystals, they also produced images of sharp, very dense lines, reminiscent of the electron-dense needle or rod-like appearances frequently observed by transmission electron microscopy of thin sections of calcified cartilage and thought to represent the habit of the apatite crystals. No true rod or needle-like crystals were observed in the isolated crystals. Although the overall general apatitic structure of the apatite crystals was similar to that of the apatitic crystals of bone, the individual crystals were significantly larger than those of bone from the same specimen, and there were small but significant differences in the concentrations of acid phosphate and carbonate groups and in their short range order.

Key words: Apatite — Crystals — Calcified cartilage.

Ultrastructural studies of thin sections of the apatite crystals of calcified cartilage by transmission electron microscopy (TEM) in many instances have revealed their habit to be needle- or rod-like, although a number of investigators have also reported the presence of thin plates ranging in size from ~30 to 80 nm in length and ~5 nm in width [1–9]. The difficulties experienced in defining the exact size and shape of the crystals inherent in all of the calcified vertebrate tissues containing small crystals of apatite [1, 10] are compounded in calcified cartilage because of the presence of large amounts of proteoglycans, the less ordered ultrastructural organization of the structural proteins and the tissue at all levels of the anatomic hierarchy, and the increased mineral density and packing of the crystals compared with bone for example [8].

To investigate the size and habit of the crystals of calcified cartilage and the short-range order of the minor but important constituents (CO_3 and HPO_4), we have utilized the reaction of hydrazine at low temperature [10, 11] to degrade most of the organic constituents in the tissue, a process that releases the crystals free of most of the organic constituents. Because most of the crystals were released by reaction with hydrazine as small aggregates of the individual crystals, the crystals were further treated by low temperature plasma ashing [10] which released single, individual crystals, although fewer than released from the same specimen of bone (diaphyseal cortex) [10]. When carried out at low temperature, the reaction with hydrazine and plasma ashing does not alter either the overall apatitic structure of the crystals or their internal short-range order [10, 11]. The crystals were found to be long rectangular plates which were significantly larger than the crystals isolated from the same bone (chicken) and from the crystals of bovine, mouse, and fish bone [10]. No rod- or needle-like crystals were observed. The dense needle-like appearance observed by TEM of thin sections arises from curved, bent, and folded plates which in addition, overlap one another.

Small but significant differences in the concentrations of HPO_4 and CO_3 groups were observed between the crystals of calcified cartilage and bone. The differences in crystal size, composition, crystallinity, and short-range order of apatite crystals in enamel, bone, and calcified cartilage support the concept that these characteristics reflect differences in the physical chemical reactivity of the crystals and consequently on the specific biological functions of the respective tissues in which they are embedded.

Materials and Methods

Animals

Lower femora of freshly slaughtered ~5–6-week-old chickens were used as the principal tissue examined. There is no secondary

**Current address:* Department of Oral Anatomy, Division of Oral Histology, College of Dentistry, Seoul National University, Seoul, Korea
Correspondence to: M. J. Glimcher

center of ossification present at the stage of development utilized and in addition, there is a sharp cleavage between the more superficial portion of the cartilaginous end of the bone and the underlying growth cartilage which participates in the sequence of endochondral ossification. With sharp cutters and a wrench-like tool, the entire articular cap can be removed, the fracture occurring roughly between the more superficial, true articular cartilage and the deeper growth cartilage which participates in endochondral ossification. Thin slices of the remaining subarticular growth cartilage were then removed parallel to the surface of the cartilage with a razor blade and frozen in liquid nitrogen. Histological sections were prepared of decalcified and undecalcified specimens of the exposed growth plate surface before and after the surface slices were removed. Cross-sections of slices and portions of the slices were also removed, as was the tissue remaining on the end of the bone after the slices were removed. For undecalcified sections, the tissues were immersed in ethylene glycol for 5 days, then in ethylene glycol monoethyl ether for 24 hours. They were then immersed in 100% ethyl alcohol 3× for 90 minutes, then embedded in catalyzed JB-4A solution for 8 weeks. For decalcified sections, tissues were fixed in 2% paraformaldehyde, 0.1 M cacodylate buffer, pH 7.4 for 12 hours, rinsed 3× for 15 minutes in 0.1 M cacodylate buffer, pH 7.4 and placed in 7.4% EDTA, 0.1 M cacodylate buffer, pH 7.4 at 4°C. Solution was changed daily until fully decalcified. The tissue was then dehydrated in 70–100% ethanol (EtOH) and infiltrated. The sections were either processed in paraffin or in JB-4A solution, stained with toluidine blue safranin-O and hematoxylin and eosin. Calcified sections were also stained by the von Kossa technique. These revealed that only uncalcified and calcified growth cartilage were included in the specimens removed for analysis. Calcified cartilage of the subarticular growth plate of 4–6-week old calves was also examined. In the case of calf bone, it was not possible to remove an articular cap, separating the two functionally different cartilages in the subarticular growth plate. Instead, the cartilaginous condyles were cut vertically into several blocks revealing the junction between the subarticular cartilage and the underlying spongiosa of bone. Very thin slices of the articular cartilage and the underlying uncalcified subarticular growth cartilage were carefully removed. The deeper layers, which by histological examination consisted only of uncalcified and calcified subarticular growth cartilage but no bone, were collected and the samples frozen in liquid nitrogen. Because the isolated crystals from calcified bovine cartilage were extracted almost entirely as aggregates of individual crystals, and even after plasma ashing yielded fewer isolated individual crystals, only TEM and limited X-ray and electron diffraction and Fourier transform infrared spectroscopy (FTIR) studies were carried out on crystals extracted from bovine calcified cartilage.

Preparation and Examination of Crystals by Electron Microscopy

Individual crystals and small crystal aggregates were isolated by a modification of methods previously described [10, 11]. Briefly, defatted cartilage powder was treated with anhydrous hydrazine (Sigma) (10 mg/10 ml) for 12–24 hours at 4°C with continuous stirring and intermittent low power ultrasonication for 5–15 minutes every 2 hours. In some instances, this procedure was repeated once. Because most of the crystals released by reaction with hydrazine were in the form of small clusters of individual crystals, the crystal preparation was further treated with low temperature plasma ashing [10] which resulted in the eventual isolation of individual crystals, although the relative number of isolated crystals was significantly less than was isolated from bone of the same specimen (diaphysis) [10]. Isolated crystals and crystal aggregates were placed on carbon-coated formvar supported grids and examined in a JEOL 100 C TEM equipped with a liquid nitrogen-cooled stage to minimize temperature-induced artifacts and contamination of the sections. The maximum length and width of the isolated individual crystals and crystals in small aggregates whose outlines were visible were digitized using a digitizer (0.1 mm resolution) attached to a personal computer. The measurements of maximum length and width were carried out on individual crystals lying flat on the gird at a magnification of ×102,000. With the aid of stereograms and goniometer tilting of the stage, one could confirm that the crystals measured were lying flat on the grids. Accurate determination of the thickness of the crystals was not possible due to the fact that they were extremely thin, and the fact that crystals were often bent and curved so that it was impossible to get a real edge-on view.

X-ray and Electron Diffraction Analysis

The long-range order of the isolated crystals was determined by powder X-ray diffraction using CU Kα-radiation (80 KV, 40 mA). Electron diffraction was carried out using a JEOL 100C electron microscope fitted with a liquid cooling N_2 cooling device. X-ray, electron probe microscopic analysis was carried out using a JEOL model 1210 at 80 KV and ~5A with attached Voyager emission 3 X-ray microprobe analyzer (Noran, Instruments, Inc., Middleton, WI 53562).

Fourier Transform Infrared Spectroscopy

Characteristics of the short-range order of the mineral phase in cartilage crystals were assessed by computer, resolution-enhanced deconvoluted FTIR on a Perkin Elmer 1700 spectrometer. Deconvolution of the FTIR spectra was obtained using the constructor software. The sensitivity coefficients and the bandwidths are reported in the figure legends. Intensity ratios and resolution factors were calculated as previously reported [12].

Results

After reaction with hydrazine, the crystals were released from the cartilage principally as small aggregates. In stereograms obtained after extensive reaction with hydrazine and plasma ashing, the packing and the shape of individual crystals were clearly seen (Fig. 1A–C). The crystals were extremely thin, wide, relatively long rectangular plates (Table 1). They were significantly larger than the crystals of bone isolated from the same bone and from the bone of three other species [10]. The packing arrangement of the individual crystals in small aggregates was clearly observed in the stereograms. A most interesting feature of the crystal habit was that most of the individual crystals in the crystal aggregates were curved and/or bent or folded, and many crystals were twisted on themselves to varying degrees. The rod- or needle-like high density appearance generated by the bending, twisting, and physical overlapping of the crystals in the aggregates and the low density of the thin crystals or that portion of the crystals lying flat on the grid, produced the appearance of electron optically dense "needles" or "rods." The dense appearance of most of the rod or needles made it appear that the apparent needle-like crystals were thicker than they actually were, viz., the determination of the true thickness of the crystals was impossible because the edge-on view of the crystals did not reflect the true thickness of the crystals. Electron diffraction of individual crystals or clusters identified the crystals as apatite (Fig. 2A–C). The crystals in the clusters, especially the largest ones, tended to show a random orientation, although in a few instances most of the crystals in a cluster were oriented with their c-axes relatively parallel with one another. In other instances, it was not possible to distinguish whether the apparent randomization of the c-axes, or in some cases the recording of more than one c-axis orientation, was due in part to folding or bending of several individual crystals.

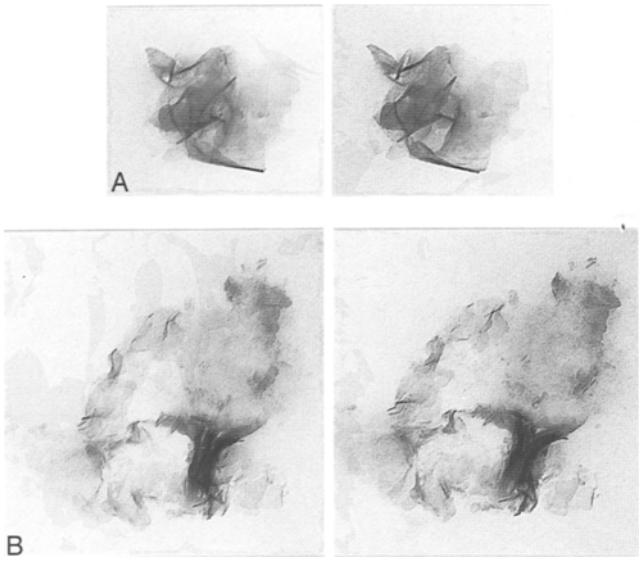

Fig. 1. Electron micrographs of crystal aggregates isolated from **(A)** stereograms of chicken and **(B)** bovine calcified cartilage. The long and wide large plates, some of which are curved, bent, folded, and overlapped with adjacent crystals are clearly seen. Some crystals are oriented vertically to the flat crystals. The electron-dense lines suggestive of rod- or needle-like crystals do not represent an edge on view of plates or of dense needle- or rod-like crystals but result principally from optically bent, curved, and overlapped crystals (±8° tilt, ×102,000). **(C)** When lying flat, crystals are thin, based on minimal electron density ×95,000.

Table 1. Size of crystals of calcified subarticular growth plate cartilage of chickens (nm)

	Length	Width	Thickness
Average ± SD[a]	103 ± 26	68 ± 16	N.D.[1]
Size range	70 – 160	40 – 100	—

[1] See text
[a] n = 25

Electron probe microanalysis of individual clusters of crystals showed a typical pattern of calcium-phosphate apatite (Fig. 2D). The basic habit of the crystals of chicken and bovine cartilage was similar, but the aggregates of the bovine crystals were generally larger than those of chicken cartilage. It should be noted that unlike bone, it was difficult to isolate large numbers of individual crystals even by plasma ashing after treatment with hydrazine which removed essentially all of the organic matrix constituents (less than 0.5% remaining).

X-ray diffraction identified the crystals as apatite. No other calcium-phosphate mineral phase was detected either by X-ray diffraction (Fig. 3) or FTIR (Figs. 4–6).

The overall deconvoluted FTIR spectrum of hydrazine-reacted crystals of chicken cartilage (Fig. 4) shows the typical spectra bands observed in young crystals of apatite in bone [10, 12, 13]. In addition, the presence of amide bands, especially at 1520 cm^{-1}, clearly indicates the presence of residual organic constituents after treatment with hydrazine alone. The band at 1230 cm^{-1} represents residual proteoglycan. The low intensity of the carbonate band at 870 cm^{-1} compared with the phosphate bands is indicative of a low carbonate content. In the ν_4 phosphate domain, the major spectrum band is assigned to PO_4 ions in apatitic sites. The spectra band at 545 cm^{-1} assigned to HPO_4 is very likely in an apatitic environment. Several nonapatitic phosphate bands are also seen: the 530 cm^{-1} band representing HPO_4 ions in nonapatitic sites and the 615 cm^{-1} band representing phosphate (possibly PO_4) also in nonapatitic sites.

Similarly, the FTIR spectra in the ν_2 carbonate domain (Fig. 6) exhibit the characteristic three distinct bands which are also seen in bone crystals [10, 14]. These bands at 879, 873, and 866 cm^{-1} are assigned, respectively, to type A carbonate (carbonate ions substituted for OH ions in hydroxyapatite), type B carbonate (carbonate ions substituting for phosphate ions), and as labile, nonapatitic carbonate ions probably located principally on the surfaces of the crystals [15–19]. Though the spectra in general are similar to those observed in young bone crystals, there are significant differences between the spectra generated by the young cartilage crystals and those generated by young bone crystals. These include a much lower total concentration of carbonate ions in the cartilage crystals than in the bone crystals, but a higher proportion of labile nonapatitic CO_3 relative to the total CO_3 content. Indeed, the cartilage crystals contained more labile components (CO_3 and phosphate) in nonapatitic sites than in bone crystals. These observations combined with the fact that the CO_3 bands are not as well resolved as the CO_3 bands in bone crystals suggest that the CO_3 ions in cartilage crystals are preferentially distributed in less ordered atomic environments (less order in the short-range structure). Similar observations have been made in young apatite crystals formed *in vitro* [12–17]. The ratio of type A/type B CO_3 positions (0.62) is significantly lower than in chicken bone (0.75–0.8). Since this ratio is quite constant during the maturation of bone crystals, it suggests that the conditions during crystal formation and maturation are different in chicken cartilage than in bone even in the case of the youngest crystals of bone. Similar results have been obtained previously for growth cartilage of bovine scapulae and of bovine bone from the same scapulae [18].

Although there is some analogy with the spectra generated by the cartilage crystals with those generated by octacalcium phosphate (OCP), as already noted in a previous study [19], there are several shifts in the spectral band positions compared with the spectra generated by OCP. Importantly, the specific spectral band typical of OCP at 917 cm^{-1} was not detected. These data indicate that no solid phase of *crystalline* OCP is present in the calcified cartilage of chickens, even in the youngest crystals (mineral content of starting tissue ~3–4%). Similar results were obtained previously [18] and in the present study from bovine calcified cartilage.

Discussion

One of the prevalent views concerning the habit of the apatite crystals of calcified cartilage is that they are needle- or rod-like [3–7]. This is not borne out by the present study utilizing direct TEM of isolated aggregates and individual crystals essentially free of organic matrix constituents; the crystals are thin, relatively long rectangular plates, significantly larger than bone crystals isolated from the same bone and from four different species [10, 11]. There was no evidence for the presence of needle- or rod-like crystals. The rectangular, plate-like habit of the crystals is consistent with

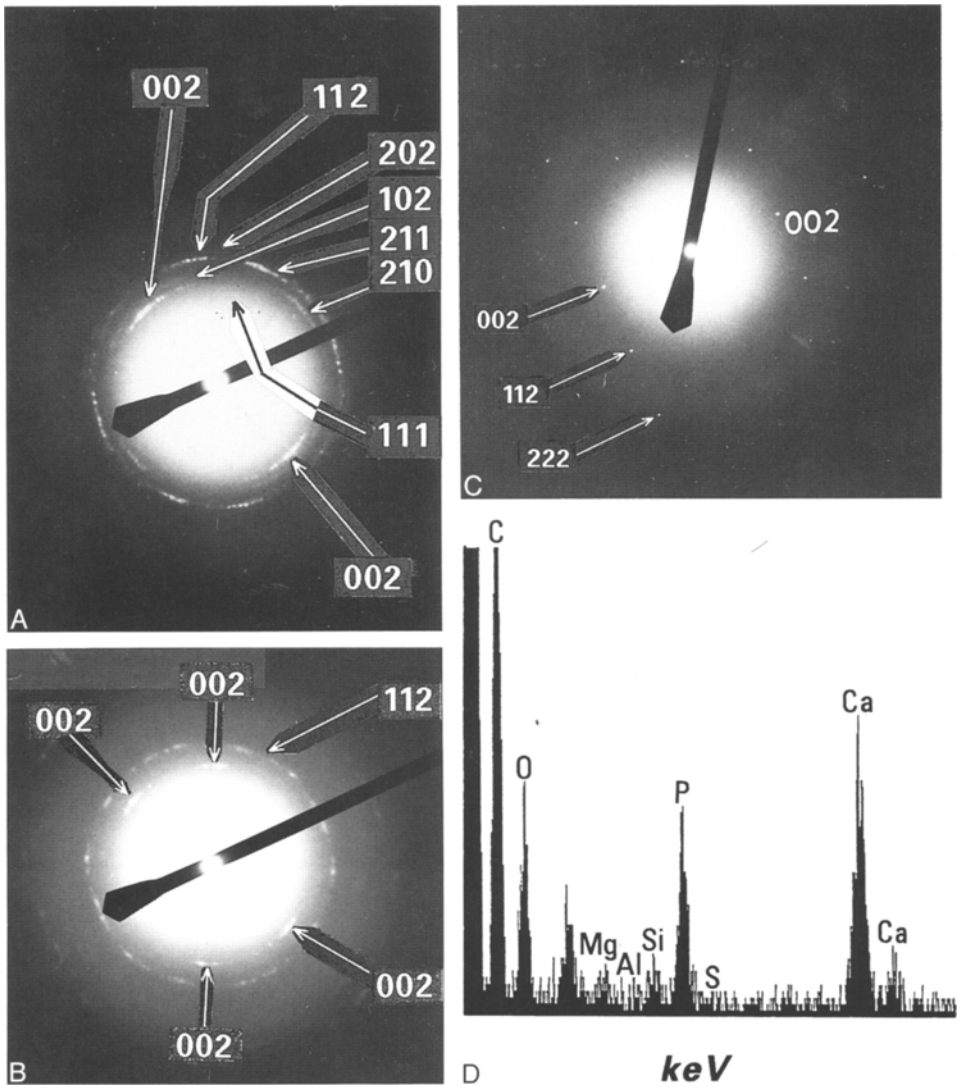

Fig. 2(A) Electron diffraction pattern generated from an aggregate of individual crystals of calcified chicken cartilage. Preferred orientation of the c-axes of the crystals (002 reflections) and of the 210 reflections indicate that these crystals in this particular aggregate, which are lying sufficiently flat on the grid so that their c-axes and the 210 reflections can be diffracted, are preferentially oriented with respect to their crystallographic C-axis (long axes). However, the presence of random 112, 202, 211, and 111 reflections indicate that there are other crystals in the aggregate which are not lying perpendicularly enough to the electron beam to generate c-axes reflections and whose c-axes are not similarly oriented as those crystals generating the c-axis reflections, viz., crystals oriented at various angles to the crystals lying flat on the grid. Similar results would be obtained from bent or folded crystals. **(B)** Electron diffraction of an aggregate of crystals from calcified chicken cartilage. Note two distinct c-axis orientations. It is not possible to determine from the X-ray diffraction patterns alone how much of the two distinct c-axis directions is due to differences in the c-axis orientations of individual crystals and how much is due to the bending and folding of individual crystals. The random 112 reflections cannot be generated from two sets of crystals lying flat on the grid with their c-axes oriented at a distinct angle to one another. **(C)** Electron diffraction pattern from a large single crystal from calcified cartilage of chicken. The single crystal pattern even from such a large crystal establishes that the large crystals are not an aggregate of smaller crystals. **(D)** Electron probe microanalysis of an aggregate of single crystals from chicken cartilage. Major constituents are Ca and P with relative intensities consistent with composition of apatites.

the findings of others [2, 8] although these investigators suggested that the large crystal plates were composed of smaller particles. We did not find any evidence for smaller particles and indeed electron diffraction of even the largest, individual, isolated crystals generated single crystal patterns, firmly establishing that the large individual crystals were indeed single crystals and not aggregates of much smaller particles. Electron diffraction of relatively large clusters of crystals generated interrupted ring reflections which also demonstrate that the large aggregates consisted of a relatively small number of large crystals. Since the calcified cartilage was initially obtained from the early stages of calcification (less than ~3% mineral content), additional studies were carried out on deeper portions of the calcified cartilage. The results were similar. The failure to detect needle- or rod-like crystals casts some question on the postulated morphological or functional relationship between the crystals and the dense needle-like appearance of the organic matrix of decalcified and uranyl acetate or lead citrate-stained calcified cartilage (''crystal ghosts'') [3–7],

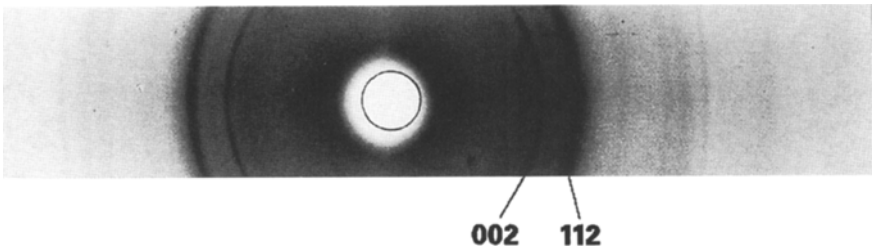

Fig. 3. X-ray diffraction of crystals isolated from calcified chicken cartilage by reaction with hydrazine. Similar diffractograms were obtained following plasma ashing after hydrazine reaction. X-ray diffractograms obtained from isolated crystals of calcified bovine cartilage were similar to those from crystals of calcified cartilage of chicken.

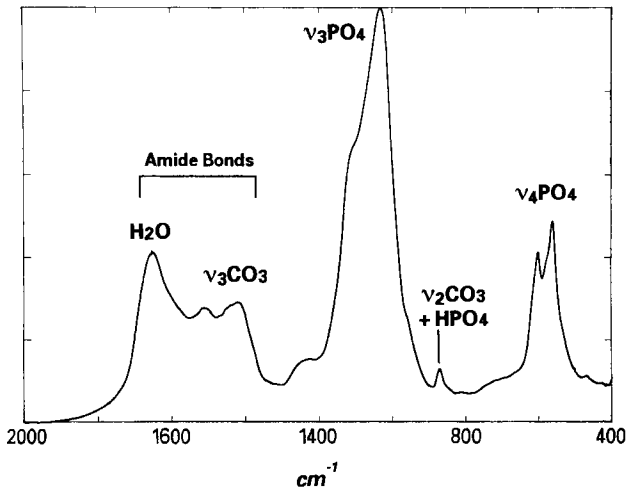

Fig. 4. General FTIR spectrum of apatite crystals of calcified cartilage of chicken isolated by reaction with hydrazine.

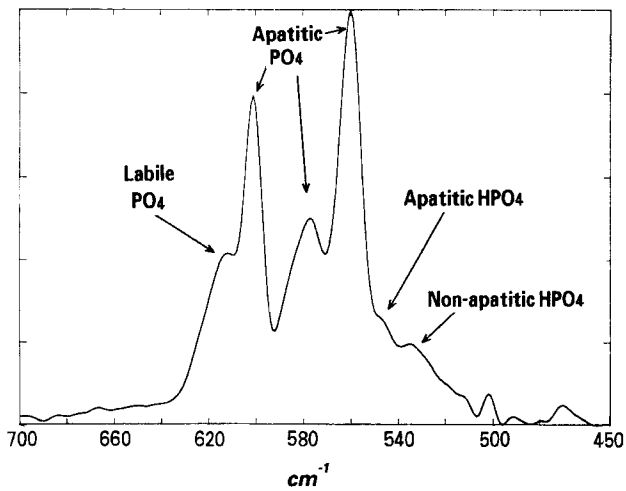

Fig. 5. Deconvoluted FTIR spectrum in the ν_4PO_4 domain of apatite crystals of calcified cartilage of chicken isolated by hydrazine followed by low temperature plasma ashing. In addition to apatitic PO_4 environments, labile nonapatitic environments are also present. Deconvolution parameters: band width 18 cm^{-1}; sensitivity coefficient 2.25.

at least on the basis of their purported morphological similarity. The presence of bent or partially folded crystals of apatite from tooth enamel has been clearly identified both *in situ* and in isolated crystals of apatite [23–25]. From a review of numerous electron micrographs of thin sections of calcified cartilage ([1–8] for example), as well as our own [9], it appears likely that the same holds true of the crystals of calcified cartilage, viz., that the needle-like appearances of the crystals is for the most part due to folding and bending of thin individual crystals closely aggregated. A few of the thinnest dense "lines" may be attributed to end on view of plates.

The strong tendency of the crystals to aggregate and the difficulty in isolating single crystals even after plasma ashing when the protein content of the crystals was reduced to less than 1–2%, suggests that the residual organic matrix constituents may be bound and trapped between the surfaces of individual crystals and are not wholly accessible to either the hydrazine or the plasma ashing.

Although the crystals of bone and cartilage are basically apatite, there are differences in their short-range order and composition with respect to the important minor constituents, HPO_4 and CO_3 ions. During the past decade or so, work on the crystalline mineral phase of the calcified tissues of vertebrates has focused on the subtle differences in the size, shape, and composition of the important minor components HPO_4 and CO_3 of the crystals, as well as differences in the short-range order of the crystals in the various tissues. Most recently, these studies have advanced to the stage where light microscopic infrared spectroscopy has been successfully used in calcified tissue sections to determine the local relative concentrations of the mineral phase and the relative local intensities of the CO_3 and HPO_4 ions [20–22]. The present report adds to this body of information and is consistent with the proposal that the physical chemical reactivity of the crystals which is highly dependent on the crystal size, habit, composition of important minor constituents, and their local environment and short range order may account for some of the differences in their biological functions in the different calcified tissues. This is consistent with one of the major current basic tenets of biology, namely, that the specific biological functions of organic matrix constituents such as proteins are specifically related to their precise composition and three-dimensional molecular configuration, and in many cases to their exact macromolecular packing and aggregation, as well. The same dependence of function on structure is also likely to be true of the inorganic crystalline phase as well.

Acknowledgments. This work was supported in part by NIH grants AR34081 and PO1-AR3478, a grant from the Peabody Foundation, and an Orthopaedic Research and Education Foundation Institutional Grant funded by the Bristol-Meyers Squibb/Zimmer

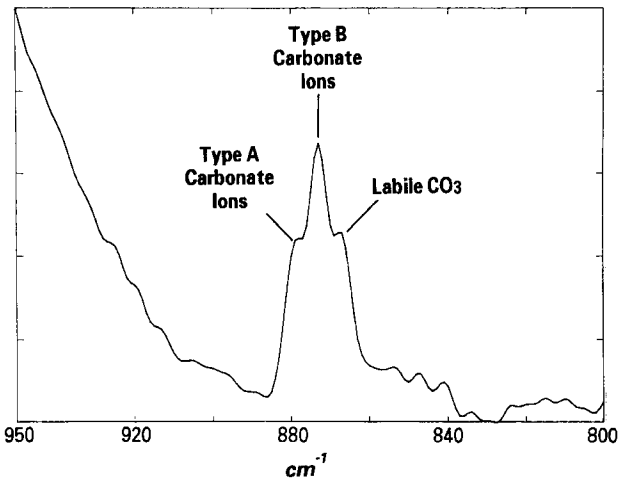

Fig. 6. Deconvoluted FTIR spectrum in the ν_4CO_3 domain of apatite crystals of calcified cartilage of chicken followed by plasma ashing. Carbonate ions are located in both anionic sites of the apatitic structure type: type A carbonate-apatite (CO_3 substituted for OH groups) and type B carbonate-apatite (CO_3 substituted for PO_4 groups). In addition, a labile non-apatitic CO_3 environment is also present. Deconvolution parameters: band width 10 cm^{-1}; sensitivity coefficient 2.25.

Corporation. The authors wish to acknowledge the expert editorial assistance of Ms. Lisa Lagasse and Ms. Carolyn Gregory. We would like to thank Mr. Dave Harling and the JEOL, USA Company, Peabody, MA for their help with the electron microscopy, electron diffraction, and electron probe X-ray microanalyses of several of the samples using the JEOL model 1210 with attached Voyager Emission 3 X-ray analyzer (Noran Instruments, Inc.). Finally, we also wish to thank Mr. Richard Kyle, 5000K Digital Studio, Inc., Boston, MA for his expert photographic assistance in preparing the single crystal electron diffraction pattern.

References

1. Arsenault AR, Hunziker EB (1988) Electron microscopic analysis of mineral deposits in the calcifying epiphyseal growth plate. Calcif Tissue Int 42:119–126
2. Arsenault AR, Grynpas MD (1988) Crystals in calcified epiphyseal cartilage and cortical bone of the rat. Calcif Tissue Int 43:219–225
3. Bonucci E (1967) Fine structure of early calcification. J Ultrastruct Res 20:33–50
4. Bonucci E (1969) Further investigation on the organic/inorganic relationships in calcifying cartilage. Calcif Tissue Int 3:38–54
5. Bonucci E, Silvestrini G, DiGrezia R (1988) The ultrastructure of the organic phase associated with the inorganic substance in calcified tissues. Clin Orthop 233:243–261
6. Bonucci E, Silvestrini G, di Grezia R (1989) Histochemical properties of the "crystal ghosts" of calcifying epiphyseal cartilage. Connect Tissue Res 22:43–50
7. Bonucci E (1992) Comments on the ultrastructural morphology of the calcification process: an attempt to reconcile matrix vesicles, collagen fibrils and crystal ghosts. Bone Miner 17: 219–222
8. Hunziker ET, Hermann W, Cruz-Orive LM, Arsenault AL (1989) Image analysis of electron micrographs relating to mineralization in calcifying cartilage: theoretical considerations. J Electron Microsc 11:9–15
9. Landis WJ, Glimcher MJ (1982) Electron optical and analytical observations of rat growth plate cartilage prepared by ultracryomicrotomy: the failure to detect a mineral phase in matrix vesicles and the identification of heterodispersed particles as the initial solid phase of calcium phosphates deposited in the extracellular matrix. J Ultrastruct Res 78:227–268
10. Kim H-M, Rey C, Glimcher MJ (1995) Isolation of calcium-phosphate crystals of bone by non-aqueous methods at low temperature. J Bone Miner Res 10:1589–1601
11. Kim H-M, Rey C, Glimcher MJ (1994) Isolation of calcium-phosphate crystals of mature bovine bone by reaction with hydrazine at low temperature. In: Brown P (ed) Hydroxyapatite and related materials. CRC Press, Boca Raton, FL, pp 331–338
12. Rey C, Shimizu M, Collins B, Glimcher MJ (1990) Resolution-enhanced Fourier transform infrared spectroscopy study of the environment of phosphate ion in the early deposits of a solid phase of calcium phosphate in bone and enamel and their evolution with age. I. Investigations in the ν4PO4 domain. Calcif Tissue Int 46:383–393
13. Rey C, Shimizu M, Collins B, Glimcher MJ (1991) Resolution-enhanced Fourier transform infrared spectroscopy study of the environment of phosphate ions in the early deposits of a solid phase of calcium phosphate in bone and enamel and their evolution with age: 2. Investigations in the ν3PO4 domain. Calcif Tissue Int 49:383–388
14. Rey C, Collins B, Goehl T, Dickson IR, Glimcher MJ (1989) The carbonate environment in bone mineral: a resolution-enhanced Fourier transform infrared spectroscopy study. Calcif Tissue Int 45:157–164
15. Rey C, Kim H-M, Glimcher MJ (1994) Maturation of poorly crystalline synthetic and biological apatites. In: Brown PW, Constantz B (eds) Hydroxyapatite and related materials. CRC Press, Boca Raton, FL, pp 181–187
16. Rey C, Hina A, Glimcher MJ (1996) Maturation of poorly crystalline apatites: chemical and structural aspects, in vivo, and in vitro behavior. Cells Materials (in press)
17. Rey C, Glimcher MJ (1992) Short-range organization of the Ca-P mineral phase in bone and enamel: changes with age and maturation. In: Slavkin H, Price P (eds) Chemistry and biology of mineralized tissues. Elsevier, Amsterdam, pp 5–18
18. Rey C, Beshah K, Griffin R, Glimcher MJ (1991) Structural studies of the mineral phase of calcifying cartilage. J Bone Miner Res 6:515–525
19. Rey C, Miquel JL, Facchini L, Legrand AP, Glimcher MJ (1995) Hydroxyl groups in bone mineral. Bone 16:583–586
20. Pleshko N, Mendelsohn R, Boskey AL (1992) Developmental changes in bone mineral: an FT-IR microscopy study. Calcif Tissue Int 51:72–77
21. Boskey AL, Pleshko N, Binderman I, Mendelsohn R (1992) Mineralization during in vitro calcification: an FT-IR microscopic mapping of early mineralization in chicken limb bud mesenchymal cell cultures. Calcif Tissue Int 51:443–448
22. Boskey AL, Pleshko N, Doty SB, Mendelsohn R (1992) Applications of FT-IR microscopy to the study of mineralization in bone and cartilage. Cells Materials 2:209–220
23. Warshawsky H, Nanci A (1982) Stereo microscopy of enamel crystallites. J Dent Res 61:1504–1514
24. Warshawsky H, Bai P, Nanci A (1987) Analysis of crystallite shape in rat incisor enamel. Anat Rec 218:380–390
25. Dong W (1993) Normal bending of crystallites in rat incisor enamel revealed by freeze-fracture replicas, isolated enamel crystallites and high-resolution electron microscopy. In: Ultrastructural studies of crystallite formation and organization in rat incisor enamel and shark enameloid. Ph.D. Thesis. McGill University, Montreal, Canada